



**Heriot-Watt University**

Heriot-Watt University  
Research Gateway

## **Quantum Zeno control of decoherence**

Maniscalco, Sabrina

*Published in:*  
Laser Physics

*DOI:*  
[10.1134/S1054660X10090094](https://doi.org/10.1134/S1054660X10090094)

*Publication date:*  
2010

[Link to publication in Heriot-Watt Research Gateway](#)

*Citation for published version (APA):*  
Maniscalco, S. (2010). Quantum Zeno control of decoherence. *Laser Physics*, 20(5), 1251-1261.  
[10.1134/S1054660X10090094](https://doi.org/10.1134/S1054660X10090094)



### **General rights**

Copyright and moral rights for the publications made accessible in the public portal are retained by the authors and/or other copyright owners and it is a condition of accessing publications that users recognise and abide by the legal requirements associated with these rights.

If you believe that this document breaches copyright please contact us providing details, and we will remove access to the work immediately and investigate your claim.

# Quantum Zeno Control of Decoherence<sup>1</sup>

S. Maniscalco

*Turku Centre for Quantum Physics, Department of Physics and Astronomy, University of Turku,  
FI-20014, Turku, Finland*

e-mail: [sabrina.maniscalco@utu.fi](mailto:sabrina.maniscalco@utu.fi)

Received October 24, 2009; in final form, November 5, 2009; published online April 2, 2010

**Abstract**—We demonstrate the possibility of controlling the quantum to classical transition by means of the quantum Zeno and anti-Zeno effects. We consider a quantum harmonic oscillator initially prepared in a Schrödinger cat state and interacting with an engineered amplitude reservoir. We show that the environment induced decoherence transforming the cat state into a statistical mixture can be strongly inhibited by means of either appropriate sequences of measurements or shuttered reservoirs.

DOI: 10.1134/S1054660X10090094

## 1. INTRODUCTION

The increasing ability in coherent control and manipulation of the state of quantum systems has paved the way to experiments able to monitor the transition from quantum superpositions, such as the paradigmatic Schrödinger cat states, to classical statistical mixtures [1, 2]. The emergence of the classical world from the quantum world, due to decoherence induced by the environment, has been extensively investigated in the last few decades both in connection to fundamental issues of quantum theory and in relation to the emerging quantum technologies. The fragile nature of quantum superpositions and entangled states exploited, e.g., in quantum communication, quantum computation, and quantum metrology, makes these potentially very powerful techniques also very delicate. For this reason several methods have been proposed in order to protect quantum states from decoherence and dissipation. For example, methods based on decoherence free subspaces, dynamical decoupling and bang-bang techniques, just to mention a few, have been investigated [3]. Recently the connection between these techniques and the quantum Zeno effect has been clarified [4].

In a recent Letter we have studied the conditions for observing the Zeno and anti-Zeno effects in a damped harmonic oscillator [5]. The quantum Zeno and anti-Zeno effects [6, 7] predict, respectively, the inhibition and the enhancement of the decay of the initial state due to a series of measurements aimed at checking whether the system is still in its initial state or not [8]. Typically, when studying Zeno and anti-Zeno dynamics, the system is assumed to be initially prepared in an eigenstate of the free Hamiltonian, e.g., in our case, a Fock state. This is the situation we have considered in [5, 9]. The aim of this paper is to see whether the quantum Zeno effect can be exploited also to inhibit quantum decoherence when the system

is initially prepared in a Schrödinger cat state. The analysis of Zeno and anti-Zeno phenomena in the context of the damped harmonic oscillator gives us the possibility of exploring the modification of the quantum-classical transition as an effect of measurements performed on the system. This possibility stems from the fact that the harmonic oscillator possesses both quantum states, such as Fock states and superposition of coherent states, and classical (or semiclassical) states, such as the coherent and the thermal states.

Another aspect discussed in the paper is the connection between the dynamics in presence of non-selective energy measurements and the dynamics in presence of modulation of the system-reservoir coupling constant. The second scenario may be useful in implementing experiments aimed at revealing the quantum Zeno and anti-Zeno effects with engineered reservoirs [1, 2]. We will show that, for certain types of reservoirs, a simple periodic modulation of the system-reservoir coupling constant is equivalent to performing non-selective energy measurements, as one would expect from the results presented in [4]. An experimental verification of the Zeno and anti-Zeno effects with engineered reservoirs would allow one to observe these phenomena through indirect measurements, contrarily to the direct ones of [10], in the spirit of the “genuine” quantum Zeno effect [11].

The outline of the paper is the following. In Section 2 we describe the non-Markovian dynamics of the damped harmonic oscillator and we present the master equation and its solution in terms of the Wigner function. In Section 3 we show how the dynamics changes both in presence of non-selective energy measurements performed on the system and in the case of a shuttered reservoir. Section 4 contains the main result of the paper, i.e., the possibility of controlling the quantum-classical border using quantum Zeno phenomena. Finally, Section 5 contains the conclusions.

<sup>1</sup> The article is published in the original.

## 2. THE SYSTEM

### 2.1. The Master Equation

We consider a harmonic oscillator linearly coupled to an engineered reservoir modelled as an infinite chain of non-interacting oscillators [12–18]. The microscopic Hamiltonian of the total system, in units of  $\hbar$ , has the form

$$H = H_0 + H_E + H_{\text{int}}, \quad (1)$$

$$H_0 = \omega_0 \left( a^\dagger a + \frac{1}{2} \right), \quad (2)$$

$$H_E = \sum_n \omega_n \left( b_n^\dagger b_n + \frac{1}{2} \right), \quad (3)$$

$$H_{\text{int}} = g \sum_n \kappa_n (a^\dagger + a) (b_n^\dagger + b_n), \quad (4)$$

where  $H_0$ ,  $H_E$ , and  $H_{\text{int}}$  are the system, environment and interaction Hamiltonians, respectively,  $a$  ( $a^\dagger$ ) and  $b_n$  ( $b_n^\dagger$ ) are the annihilation (creation) operators of the system and of the reservoir quantum oscillators, respectively,  $\omega_0$  is the frequency of the system oscillator,  $\omega_n$  are the frequencies of the reservoir oscillators,  $g$  is the coupling constant, and the quantities  $\kappa_n$  describe how strongly the reservoir oscillators are coupled to the system. In the continuum limit  $\kappa_n$  enter in the definition of the spectral density of the reservoir, the key quantity governing the open system dynamics:  $J(\omega) = \sum_n \kappa_n \delta(\omega - \omega_n) / (2m_n \omega_n)$ , with  $m_n$  masses of the environmental oscillators [13].

Following the standard derivation of the master equation for the reduced system [see, e.g., [13]] one can demonstrate that the exact master equation, in the interaction picture, takes the form [18–20]

$$\begin{aligned} \frac{d\rho(t)}{dt} = & -\Delta(t)[X, [X, \rho(t)]] \\ & + \Pi(t)[X, [P, \rho(t)]] + \frac{i}{2}r(t)[X^2, \rho(t)] \\ & - i\gamma(t)[X, \{P, \rho(t)\}], \end{aligned} \quad (5)$$

where  $\rho(t)$  is the reduced density matrix,  $X = (a + a^\dagger)/\sqrt{2}$  and  $P = i(a^\dagger - a)/\sqrt{2}$ .

The master equation given by Eq. (5), being exact, describes also the non-Markovian short time system-reservoir correlations due to the finite correlation time of the reservoir. In contrast to other non-Markovian dynamical systems, this master equation is local in time, i.e., it does not contain memory integrals. All the non-Markovian character of the system is contained in the time dependent coefficients appearing in the master equation (for the analytic expression of the

coefficients see, e.g., [21]). These coefficients depend uniquely on the form of the reservoir spectral density. The coefficient  $r(t)$  describes a time dependent frequency shift,  $\gamma(t)$  is the damping coefficient,  $\Delta(t)$  and  $\Pi(t)$  are the normal and the anomalous diffusion coefficients, respectively [18].

The dynamics of the system has been extensively studied numerically using the path integral approach (see [17, 22] for a review). In particular, this model has been used to demonstrate the action of environment induced decoherence for initial Schrödinger cat states such as, e.g.,

$$|\Psi\rangle = \frac{1}{\sqrt{N}} (|\alpha\rangle + |-\alpha\rangle), \quad (6)$$

where  $|\alpha\rangle$  is a coherent state,

$$N^{-1} = 2[1 + \exp(-2|\alpha|^2)], \quad (7)$$

and we take  $\alpha \in \mathbb{R}$  for simplicity. It has been proven that the decoherence induced by the environment acts in a much faster time scale than the thermalization process, in particular the decoherence time  $\tau_d$  is inversely proportional to the separation between the two components of the superposition, i.e.,  $2|\alpha|^2$ . The aim of our paper is to study if and when it is possible to inhibit this fast decoherence process by means of the quantum Zeno effect.

We begin by noticing that, under certain conditions, it is possible to obtain simple analytical results for the time evolution of the density operator. In particular, for an Ohmic reservoir described by a spectral distribution of the form [12]

$$J(\omega) = \frac{2\omega}{\pi} \frac{\omega_c^2}{\omega_c^2 + \omega^2}, \quad (8)$$

with  $\omega_c$  the cutoff frequency, in the limit of high temperatures and for sufficiently weak system-reservoir couplings, both the anomalous diffusion term  $\Pi(t)$  and the frequency shift term  $r(t)$  are negligible [19, 23]. In this case, and for times  $t \ll t_{\text{th}}$ , with  $t_{\text{th}}$  the thermalization time, Eq. (5) can be approximated by the following master equation

$$\begin{aligned} \frac{d\rho(t)}{dt} = & \frac{\Delta(t) + \gamma(t)}{2} [2a\rho(t)a^\dagger - a^\dagger a\rho(t) - \rho(t)a^\dagger a] \\ & + \frac{\Delta(t) - \gamma(t)}{2} [2a^\dagger \rho(t)a - aa^\dagger \rho(t) - \rho(t)aa^\dagger] \\ & + \frac{\Delta(t) - \gamma(t)}{2} e^{-2i\omega_0 t} [2a\rho(t)a - a^2 \rho(t) - \rho(t)a^2] \\ & + \frac{\Delta(t) - \gamma(t)}{2} e^{2i\omega_0 t} [2a^\dagger \rho(t)a^\dagger - (a^\dagger)^2 \rho(t) - \rho(t)(a^\dagger)^2]. \end{aligned} \quad (9)$$

We are interested in the dynamics over time scales  $t \leq \tau_d \ll t_{\text{th}}$ . This justifies the use of the master equation (9) throughout the paper. In the next section we will

present the solution of this master equation in terms of the Wigner function and discuss its properties for an initial state of the form of Eq. (6). Moreover, we will check the validity of the approximations under which the master equation (9) holds by comparing the solution we have derived with the solution of the exact Hu-Paz-Zhang master equation (5).

The second order expansion of the diffusion and dissipation coefficients appearing in Eq. (9) reads as follows [18, 21]

$$\Delta(t) = g^2 \int_0^t \int_0^\infty d\omega dt_1 J(\omega) [2N(\omega) + 1] \times \cos(\omega t_1) \cos(\omega_0 t_1), \quad (10)$$

$$\gamma(t) = g^2 \int_0^t \int_0^\infty d\omega dt_1 J(\omega) \sin(\omega t_1) \sin(\omega_0 t_1), \quad (11)$$

with  $N(\omega) = (e^{\hbar\omega/k_B T} - 1)^{-1}$  the average number of reservoir thermal photons,  $k_B$  the Boltzmann constant, and  $T$  the reservoir temperature. We note that, for high  $T$ , i.e.,  $N(\omega) \gg 1$ ,  $\Delta(t) \gg \gamma(t)$ . The dynamics of the coefficients  $\Delta(t)$  and  $\gamma(t)$  can be easily calculated in the high  $T$  limit inserting Eq. (8) into Eqs. (10)–(11),

$$\Delta(t) = 2g^2 k_B T \frac{r^2}{1+r^2} \{1 - e^{-\omega_c t} [\cos(\omega_0 t) - (1/r) \sin(\omega_0 t)]\}, \quad (12)$$

$$\gamma(t) = \frac{g^2 \omega_0 r^2}{1+r^2} \quad (13)$$

$$\times [1 - e^{-\omega_c t} \cos(\omega_0 t) - r e^{-\omega_c t} \sin(\omega_0 t)],$$

with  $r = \omega_c/\omega_0$ .

From these equations we see that  $\Delta(t)$  and  $\gamma(t)$  start from an initial zero value and quickly approach their constant Markovian value. Indeed for  $t \gg \tau_R = 1/\omega_R$ , with  $\tau_R$  the reservoir correlation time, the time dependent coefficients  $\Delta(t) + \gamma(t)$  and  $\Delta(t) - \gamma(t)$  become

$$\Delta(t) + \gamma(t) \approx \Gamma [N(\omega_0) + 1] \equiv \gamma_1^M, \quad (14)$$

$$\Delta(t) - \gamma(t) \approx \Gamma N(\omega_0) \equiv \gamma_{-1}^M, \quad (15)$$

respectively, with  $N(\omega_0) = k_B T/\omega_0$  and

$$\Gamma = 2g^2 \frac{r^2}{r^2 + 1} \omega_0. \quad (16)$$

By looking at Eq. (9) one realizes immediately that, for times  $\omega_0 t \gg 1$  the last two terms average out to zero and the master equation reduces to the secular

approximated master equation used, e.g., [5, 9, 21, 24, 25]

$$\frac{d\rho(t)}{dt} = \frac{\Delta(t) + \gamma(t)}{2} [2a\rho(t)a^\dagger - a^\dagger a\rho(t) - \rho(t)a^\dagger a] + \frac{\Delta(t) - \gamma(t)}{2} [2a^\dagger \rho(t)a - a a^\dagger \rho(t) - \rho(t) a a^\dagger]. \quad (17)$$

It is known that in the weak coupling limit there exists a class of observables, e.g.,  $n = a^\dagger a$ , whose dynamics is not affected by the counter-rotating terms, i.e., by those terms neglected in the secular approximation [17, 19]. In general, however, the counter-rotating terms do contribute to the dynamics of the reduced density operator of the system, in particular in the short non-Markovian time scale we are interested in.

In the following we will focus on two specific physical regimes characterized by opposite values of the parameter  $r$ , namely the case in which  $r = \omega_c/\omega_0 \gg 1$  and the case  $r \ll 1$ . We will refer to these cases as the resonant and the off-resonant case, respectively, since for  $r \gg 1$  the frequency  $\omega_0$  of the oscillator overlaps with the spectrum of the reservoir while, for  $r \ll 1$ ,  $\omega_0$  is off-resonant with the spectrum  $J(\omega)$ . From previous studies on the dynamics of the heating function  $\langle n(t) \rangle$  we know that the system time evolution differs notably in these two regimes [21]. As we will see in Section 4, also the possibility of manipulating the quantum-classical transition by means of the quantum Zeno effect crucially depends on the value of the resonance parameter  $r$ .

To investigate the possibility of modifying the decoherence time by means of the quantum Zeno effect we need to focus on the short time non-Markovian dynamics, since generally the effect takes place when measurements are performed at times  $t \leq \tau_R$  [8]. It is worth stressing that, in the resonant case  $r \gg 1$ , for  $\omega_0 t \leq 1$ , we cannot use the secular approximated master equation since  $\omega_0 t \ll \omega_c t \leq 1$ . Therefore we should use Eq. (9). On the contrary, in the off-resonant case  $r \ll 1$ , we can focus on the dynamics for times  $1/\omega_0 \ll t \leq 1/\omega_c$ , since this is consistent with the assumption  $r = \omega_c/\omega_0 \ll 1$ , and use the simpler secular approximated master equation (17).

## 2.2. The Dynamics

We now look at the short-time dynamics of a Schrödinger cat state of the form given in Eq. (6). This state is also known as even coherent state due to the fact that only the even components of the number probability distribution are nonzero. The oscillations in the number state probability are a strong sign of the nonclassicality of this state. This and other nonclassical properties of the even coherent state, such as the negativity of the corresponding Wigner function, have been extensively studied in the literature (see, e.g., [26] and references therein). In Fig. 1 we show the

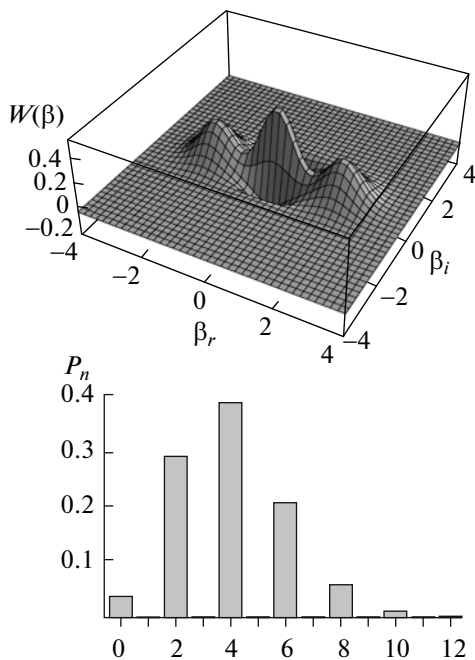


**Fig. 1.** Wigner function  $W(\beta)$  and number probability distribution  $P_n$  for the state given by Eq. (6) with  $\alpha = 2$ .

number probability distribution and the Wigner function for the even coherent state. This state has been realized in the trapped ion context and the transition from a quantum superposition to a classical statistical mixture has been observed experimentally [1].

The decoherence and dissipation due to the interaction with both thermal reservoirs and squeezed reservoirs has been studied, in the Markovian limit, in [26] and [27–29], respectively. On the other hand, the exact dynamics of the Hu–Paz–Zhang master equation (5) has been numerically investigated in [22, 23]. In the following we will look for a simple analytic solution valid in the short-time non-Markovian regime in the two limits  $r \ll 1$  and  $r \gg 1$ . We will verify the validity of the approximations made to derive such a solution comparing it with the Hu–Paz–Zhang result [22, 23].

In order to describe the transition from the initial even coherent state to the corresponding classical statistical mixture induced by the interaction with the environment it is convenient to look at the dynamics of the Wigner function. We know from the Markovian results that the quantum-classical transition is indicated by the fast disappearance of the interference fringes in the Wigner function. In order to investigate the non-Markovian dynamics we need to find out the time evolution of the Wigner function for times  $t \leq 1/\omega_c$ .

**2.2.1. The off-resonant case  $r \ll 1$ .** In the off-resonant case  $r \ll 1$  the solution of Eq. (17) in terms of the quantum characteristic function (QCF)  $\chi(\xi)$  is presented in [19]. From this solution, and remembering

that the Wigner function is the Fourier transform of the QCF,

$$W(\beta) = \frac{1}{\pi^2} \int_{-\infty}^{\infty} d^2\xi \chi(\xi) \exp(\beta\xi^* - \beta^*\xi), \quad (18)$$

one obtains straightforwardly the following expression for the dynamics of an initial even coherent state.

$$W(\beta, t) = W^{(+\alpha)}(\beta, t) + W^{(-\alpha)}(\beta, t) + W_I(\beta, t), \quad (19)$$

with

$$W^{\pm\alpha}(\beta, t) = \frac{\mathcal{N}}{\pi[N(t) + 1/2]} \exp\left(-\frac{\beta_i^2}{N(t) + 1/2}\right) \times \exp\left[-\frac{(\beta_r \mp e^{-\Gamma(t)/2}\alpha)^2}{N(t) + 1/2}\right], \quad (20)$$

$$W_I(\beta, t) = \frac{2\mathcal{N}}{\pi[N(t) + 1/2]} \exp\left(-\frac{|\beta|^2}{N(t) + 1/2}\right) \times \exp\left[-2\alpha^2\left(1 - \frac{e^{-\Gamma(t)}}{2N(t) + 1}\right)\right] \times \cos\left[\frac{2e^{-\Gamma(t)/2}}{N(t) + 1/2}\alpha\beta_i\right], \quad (21)$$

with

$$N(t) = \int_0^t dt' \Delta(t'), \quad (22)$$

$$\Gamma(t) = 2 \int_0^t dt' \gamma(t'), \quad (23)$$

where the coefficients  $\Delta(t)$  and  $\gamma(t)$  are given by Eqs. (12)–(13). As known from the Markovian theory, the interaction with the environment causes the disappearance of the interference peak and therefore the transition from quantum superposition to classical statistical mixture. An useful quantity to monitor this transition is the fringe visibility function

$$F(\alpha, t) \equiv \exp(-A_{\text{int}}) = \frac{1}{2} \frac{W_I(\beta, t)|_{\text{peak}}}{[W^{(+\alpha)}(\beta, t)|_{\text{peak}} W^{(-\alpha)}(\beta, t)|_{\text{peak}}]^{1/2}}, \quad (24)$$

where we indicate with  $W_I(\beta, t)|_{\text{peak}}$  and  $W^{\pm\alpha}(\beta, t)|_{\text{peak}}$  the value of the Wigner function at  $\beta = (0, 0)$  and  $\beta = (\pm\alpha, 0)$ , respectively. Inserting Eqs. (20)–(21) into Eq. (24) we obtain, for the  $r \ll 1$  case,

$$F(\alpha, t) = \exp\left[-2\alpha^2\left(1 - \frac{e^{-\Gamma(t)}}{2N(t) + 1}\right)\right]. \quad (25)$$

This equation tells us that, as for the Markovian theory, the interference term disappear faster and faster, the larger is the separation between the two components of the superposition, measured by  $2\alpha$ , and the higher is the temperature of the environment (see Eqs. (12)–(22)).

**2.2.2. The resonant case  $r \gg 1$ .** We now consider the dynamics in the more complicated resonant case. The solution of the master equation (9) can be obtained by noticing that this equation has the same operatorial form of the master equation for a harmonic oscillator in a thermal squeezed bath. Indeed, having in mind, e.g., [28, Eq. (6)] we can see that the two master equations coincide provided we take  $\Delta(t) + \gamma(t) = \gamma(N + 1)$ ,  $\Delta(t) - \gamma(t) \equiv \gamma N$  and  $[\Delta(t) - \gamma(t)]e^{2i\omega_0 t} \equiv -\gamma M$ . We note in passing that the condition for the positivity of the density, operator  $|M|^2 \leq N(N + 1)$  is always verified in our case. Moreover, for  $\omega_c t \leq 1$  we can approximate  $e^{2i\omega_0 t} \simeq 1$  since  $r = \omega_c/\omega_0 \gg 1$ . As a consequence we have  $M \in \mathbb{R}$  and  $M = -N$ .

In order to derive the Wigner function solution we follow the same lines of the Markovian case. We write down the Fokker-Planck equation corresponding to the master equation (9) for the Wigner function. Since the initial state is a linear combination of Gaussian terms, the form of the master equation ensures that each Gaussian term evolves independently. Therefore the evolved state will also be a linear combination of Gaussian terms [30]. Having this in mind it is straightforward to derive the Wigner function dynamics as follows

$$W^{\pm\alpha}(\beta, t) = \frac{\mathcal{N}}{\pi\{N(t) + 1/4\}^{1/2}} \times \exp\left(-\frac{\beta_i^2}{2N(t) + 1/2}\right) \exp\left[-\frac{(\beta_r \mp e^{-\Gamma(t)/2}\alpha)^2}{1/2}\right], \quad (26)$$

$$W_I(\beta, t) = \frac{2\mathcal{N}}{\pi\{N(t) + 1/4\}^{1/2}} \times \exp\left(-\frac{\beta_i^2}{2N(t) + 1/2} - \frac{\beta_r^2}{1/2}\right) \times \exp\left[-2\alpha^2\left(1 - \frac{e^{-\Gamma(t)}}{4N(t) + 1}\right)\right] \cos\left[\frac{2e^{-\Gamma(t)/2}}{2N(t) + 1/2}\alpha\beta_i\right], \quad (27)$$

with  $N(t)$  and  $\Gamma(t)$  given by Eqs. (22)–(23). Comparing the dynamics to the case  $r \ll 1$ , where the secular approximation holds, we see the following differences. First of all the variances of the two Gaussians  $W^{\pm\alpha}(\beta, t)$ , correspondent to the two components of the superposition, do not follow the same dynamics anymore. This asymmetry in the dynamics of the variances is typical of the behavior of harmonic oscillators in squeezed environments. What is more interesting for

the study of the quantum-classical transition is the behavior of the fringe visibility

$$F(\alpha, t) = \exp\left[-2\alpha^2\left(1 - \frac{e^{-\Gamma(t)}}{4N(t) + 1}\right)\right]. \quad (28)$$

Comparing this equation with Eq. (25) obtained for  $r \ll 1$  we notice that, with regard to the decoherence process, in the resonant case  $r \gg 1$  it is as if the system would interact with a thermal reservoir with an effective temperature that is the double of the real temperature. This is simply due to the non-negligible role played by the counter-rotating terms present in the microscopic interaction Hamiltonian of Eq. (4).

To conclude this section we compare the dynamics of the fringe visibility factor obtained without performing the secular approximation, i.e., by solving Eq. (9), with the result presented in [23] for the exact Hu–Paz–Zhang master equation (5). Combining Eq. (24) and Eq. (28), and using Eq. (22) we obtain

$$A_{\text{int}} = 2\alpha^2 \frac{\int_0^t 4 \int_0^{t'} dt'' \Delta(t'')}{\int_0^t 4 \int_0^{t'} dt'' \Delta(t'') + 1}, \quad (29)$$

where we have put  $e^{-\Gamma(t)} \simeq 1$  since we are far from thermalization, i.e.,  $t \ll t_{\text{th}}$ . We recall that after a time  $t \simeq \tau_R$  the diffusion coefficient attains its constant Markovian value  $\Delta_M$  and therefore  $\int_0^t dt' \Delta(t') \simeq \Delta_M t$ . Having this in mind we can compare Eq. (29) with the high temperature and low damping approximation of  $A_{\text{int}}$  given by [23, Eq. (42)]. It is immediate to notice that, mutatis mutandi, our Eq. (29) coincides with [23, Eq. (42)] for  $t \gg \tau_R$  and also it provides a straightforward generalization of this equation for the case  $t \leq \tau_R$ .

### 3. QUANTUM ZENO AND ANTI-ZENO EFFECTS FOR THE DAMPED HARMONIC OSCILLATOR

In general, quantum Zeno phenomena in unstable systems occur when repeated interruptions of the system-reservoir coupling, typically associated with measurements, modify the natural lifetime of the system [31]. It has been shown that the atomic decay into structured reservoirs can be modified by both projective (impulsive) and continuous measurements, and that it is possible to mimic the effect of both types of measurements by means of appropriate stochastic fields [31]. Furthermore, it has been demonstrated that a modulation in the system-reservoir coupling constant allows to control the decoherence and relaxation of a two-level system [32].

In a similar fashion we will now investigate the effect of both projective measurements and modula-

tion in the system-reservoir coupling constant for the damped harmonic oscillator. We will first find out when and how measurements performed on the system inhibit or enhance the decoherence of an initial Schrödinger cat state. We will then focus on the effect of a modulation of the system-reservoir coupling constant. Finally we will show when such modulation mimics the effect of a series of nonselective energy measurements performed on the system.

In the previous section we have described the non-Markovian dynamics of an even coherent state in a high  $T$  thermal bath. We have seen that due to the interaction with the environment a fast decoherence process destroys the quantumness of the initial superposition. Since we have developed a non-Markovian theory valid also for times  $t \leq \tau_R$  we can now investigate the possibility of inhibiting the decoherence process by means of the quantum Zeno effect. It is worth reminding that the quantum Zeno effect crucially relies on the short time non-Markovian behavior of the system.

In the following we will focus on the case in which the system oscillator interacts with an engineered high  $T$  reservoir. A specific implementation of a high  $T$  engineered reservoir has been demonstrated in [1, 2], in the trapped ions context. In [24] it has been shown that the engineered amplitude reservoir realized by applying noisy electric fields to the trap electrodes can be used to simulate quantum Brownian motion and that a simple modification of the experimental setup would allow to reveal the non-Markovian quadratic short time dynamics (see also [33]).

### 3.1. Evolution in Presence of Non-Selective Energy Measurements

We begin analyzing the modifications to the open system dynamics due to a series of non-selective energy measurements, described in terms of the projection operator  $\hat{P}$

$$\hat{P}\rho = \sum_n P_n |n\rangle\langle n|, \quad (30)$$

where  $|n\rangle$  are the Fock states of the harmonic oscillator and  $P_n = \langle n|\rho|n\rangle$  are the diagonal elements of the reduced density matrix [4]. Essentially the effect of these measurements is to erase instantaneously all the coherences, without selecting any of the energy states of the systems. We assume that the system oscillator interacts with an engineered reservoir and that, during the time evolution, the system is subjected to a series of nonselective energy measurements. We indicate with  $\tau$  the time interval between two successive measurements.

Following the derivation given, for a generic system, in [4] we can write down a coarse grained master

equation governing the system time evolution in presence of  $m$  nonselective measurements for  $r \gg 1$

$$\begin{aligned} \frac{d\rho(t)}{dt} = & \gamma_1(\tau)\hat{P}\left[a\hat{P}\rho(t)a^\dagger - \frac{1}{2}a^\dagger a\hat{P}\rho(t) - \frac{1}{2}\hat{P}\rho(t)a^\dagger a\right] \\ & + \gamma_{-1}(\tau)\hat{P}\left[a^\dagger\hat{P}\rho(t)a - \frac{1}{2}aa^\dagger\hat{P}\rho(t) - \frac{1}{2}\hat{P}\rho(t)aa^\dagger\right] \\ & + \gamma_{-1}(\tau)\hat{P}\left[a^\dagger\hat{P}\rho(t)a^\dagger - \frac{1}{2}aa^\dagger\hat{P}\rho(t) - \frac{1}{2}\hat{P}\rho(t)a^\dagger a^\dagger\right] \\ & + \gamma_{-1}(\tau)\hat{P}\left[a\hat{P}\rho(t)a - \frac{1}{2}a^\dagger\hat{P}\rho(t) - \frac{1}{2}\hat{P}\rho(t)a^2\right] \end{aligned} \quad (31)$$

with  $\gamma_{\pm 1}(\tau)$  given by

$$\gamma_{\pm 1}(\tau) = \tau \int_{-\infty}^{\infty} d\omega \kappa^\beta(\omega) \text{sinc}^2\left(\frac{\omega \mp \omega_0}{2}\tau\right), \quad (32)$$

where  $\text{sinc}(x) = \sin x/x$ , and the thermal spectral density  $\kappa^\beta(\omega)$  is defined as

$$\begin{aligned} \kappa^\beta(\omega) = & g^2 J(\omega)\theta(\omega)[N(\omega) + 1] \\ & + g^2 J(-\omega)\theta(-\omega)N(-\omega) \end{aligned} \quad (33)$$

with  $\theta(\omega)$  the unit step function.

For  $r \ll 1$  the master equation is given by the first two lines of Eq. (31). The dynamics described by the master equation (31) is such that only the diagonal elements of the density matrix are nonzero, due to the effect of the nonselective measurement described by Eq. (30). We note that the decay rates  $\gamma_1(\tau)$  and  $\gamma_{-1}(\tau)$  do not depend on time  $t$ , hence these rate equations are formally equivalent to those obtained from the Markovian master equation for the damped harmonic oscillator in a squeezed reservoir, provided that one identifies  $\gamma_1(\tau)$  with  $\Gamma[N(\omega_0) + 1]$  and  $\gamma_{-1}(\tau)$  with  $\Gamma N(\omega)$ . The effect of the nonselective energy measurements is therefore twofold. On the one hand they destroy the off diagonal elements of the density matrix, and on the other hand they modify the decay coefficients appearing in the rate equations in a way that depends crucially both on the system/reservoir parameters and on the interval  $\tau$  between the measurements.

An interesting feature of the system dynamics is that, due to the diagonalization of the density matrix performed by the energy measurements, the number probability distribution  $P_n(t)$  satisfies the following rate equation

$$\begin{aligned} \dot{P}_n(t) = & \gamma_1(\tau)[(n+1)P_{n+1}(t) - nP_n(t)] \\ & + \gamma_{-1}(\tau)[nP_{n-1}(t) - (n+1)P_n(t)]. \end{aligned} \quad (34)$$

Note that, the last two lines in Eq. (31), arising from the counter-rotating terms, do not contribute to the dynamics. As a consequence, Eq. (34) describes the

dynamics of the number probability distribution both in the  $r \gg 1$  regime and in the  $r \ll 1$  regime.

In order to understand in more detail how the decay coefficients are modified when compared to the Markovian ones we further investigate  $\gamma_{\pm 1}(\tau)$ , as given by Eq. (32) with Eq. (33). Recasting Eqs. (10)–(11) in the following form

$$\Delta(t) = \frac{g^2 t}{2} \int_0^\infty d\omega J(\omega) \left[ N(\omega) + \frac{1}{2} \right] \quad (35)$$

$$\times \{ \text{sinc}[(\omega - \omega_0)t] + \text{sinc}[(\omega + \omega_0)t] \},$$

$$\gamma(t) = \frac{g^2 t}{2} \int_0^\infty d\omega \frac{J(\omega)}{2} \quad (36)$$

$$\times \{ \text{sinc}[(\omega - \omega_0)t] - \text{sinc}[(\omega + \omega_0)t] \},$$

and integrating the sum and the difference of these coefficients over the time interval  $\tau$ , it is straightforward to prove that

$$\gamma_{\pm 1}(\tau) = \frac{1}{\tau} \int_0^\tau dt [\Delta(t) \pm \gamma(t)]. \quad (37)$$

The equation above shows the connection between the coefficients of the non-Markovian master equation (9) and the coefficients  $\gamma_{\pm 1}(\tau)$  modified by the presence of the nonselective energy measurements. We note first of all that when the interval between the measurements  $\tau$  is much greater than the reservoir correlation time  $\tau_R$  then  $\gamma_{\pm 1}(\tau) \approx \gamma_{\pm 1}^M$ , since  $\Delta(t)$  and  $\gamma(t)$  quickly set to their Markovian stationary values. In this case one recovers the usual Markovian dynamics, i.e., the presence of the nonselective energy measurements cannot modify the Markovian decay of the number probability distribution. Stated another way, in order to affect the dynamics one needs to perform the measurements at time intervals shorter or of the same order of the reservoir correlation time. This is well known in the theory of the quantum Zeno effect, since such effect is crucially related to the short time initial quadratic behavior of the survival probability, i.e. of the probability that a system prepared in a given initial state is still in that initial state after a time  $t$  [8].

As we mentioned before for high  $T$  reservoirs  $\Delta(t) \gg \gamma(t)$ , therefore, for times much smaller than the thermalization time  $\tau_{\text{th}} \approx 1/\Gamma$ , with  $\Gamma$  given by Eq. (16),

$$\gamma_1(\tau) \approx \gamma_{-1}(\tau) \approx \frac{1}{\tau} \int_0^\tau dt \Delta(t). \quad (38)$$

As we have noted and discussed in [5], for high  $T$  reservoirs, therefore, the modified decay rates depend only on the diffusion coefficient  $\Delta(t)$  describing environment induced decoherence. In other words the

repetition of nonselective energy measurements at short intervals  $\tau$  forces the system to experience an enhanced or reduced environment induced decoherence, depending on the form of the reservoir spectrum, and hence on the temporal behavior of  $\Delta(t)$ .

Before discussing the effect of measurements on the decoherence of an initial Schrödinger cat state, we want to address the connection between the dynamics described in this section and the situation in which the measurements are replaced by a periodic modulation in the system-reservoir coupling constant.

### 3.2. Evolution in Presence of Shuttered Reservoirs

We consider, as before, the case in which the coupling between the system oscillator and the reservoir is weak enough to justify the use of second order perturbation theory. Instead of introducing a series of nonselective energy measurements we consider the case in which the coupling between the system and the engineered reservoir is modulated as follows

$$g(t) = \begin{cases} g & \text{for } l(\tau + \delta\tau) \leq t < (l+1)(\tau + \delta\tau) \\ 0 & \text{for } l(\tau + \delta\tau) + \tau \leq t < (l+1)(\tau + \delta\tau), \end{cases} \quad (39)$$

with  $l = 0, 1, 2, \dots$ . In practice we assume that the coupling is interrupted periodically, for a short time  $\delta\tau \ll \tau$ , at intervals  $\tau$ . As we will show in the following, under certain conditions, these short interruptions mimic the nonselective energy measurements. We refer to the system described here with the name of shuttered reservoir, according to the terminology we have used in [9]. We will assume in the following that the time intervals  $\delta\tau$  are so small that the free evolution of the system can be neglected. This assumption is not necessary when we deal with the dynamics of an initial Fock state, as we have explained in [9].

Since both  $\Delta(t)$  and  $\gamma(t)$  are proportional to the coupling constant  $g$  (see Eqs. (10)–(11)), we can solve the dynamics using recursively the solution of the master equation Eq. (9). More in detail, we solve the master equation given by Eq. (9), e.g., in terms of the Wigner function, and we use the solution at time  $\tau$  as initial condition at time  $\tau + \delta\tau$ . We then calculate the solution at time  $2\tau + \delta\tau$  and use this as initial condition once more. During the time intervals  $\delta\tau$  the system oscillator is not coupled to the environment therefore its dynamics is simply given by the free evolution. If  $\delta\tau$  is such that  $0 < \delta\tau \ll 1/\omega_0$  we can neglect the system free evolution during the interval  $\delta\tau$  and assume that, at each cycle,  $\rho(\tau + \delta\tau) \approx \rho(\tau)$ . Essentially this amounts at assuming that after each time interval  $\tau$ , the “old” reservoir is replaced with a “fresh” reservoir. This is, e.g., the case for the engineered reservoir realized in the trapped ion context [2].

As noticed in [30], for the initial state we consider, the dynamics is such that each Gaussian term in the Wigner function dynamics evolves independently



always retaining its Gaussian character (see Eqs. (26)–(27)). It is therefore sufficient to follow the time dependence of the first and second statistical moments, namely the vector of first moments  $x_i = \langle X_i \rangle$ , where  $i = 1, 2$ ,  $X_1 = X$ , and  $X_2 = P$ , and the covariance matrix  $\sigma_{ij} \equiv \frac{1}{2} \langle X_i X_j + X_j X_i \rangle - \langle X_i \rangle \langle X_j \rangle$ . The covariance matrix, in our case and for  $t \leq \tau_R$ , takes the simple form

$$\sigma(t) = \begin{pmatrix} \sigma_{11}(t) & 0 \\ 0 & \sigma_{22}(t) \end{pmatrix}, \quad (40)$$

with

$$\sigma_{11}(t) \approx \sigma_{11}(0), \quad (41)$$

$$\sigma_{22}(t) \approx 2 \int_0^t dt' \Delta(t') + \sigma_{22}(0) \quad (42)$$

with  $\sigma_{11}(0) = \sigma_{22}(0) = 1/2$ . The vector of first moments is given by

$$x_i(t) = e^{-\Gamma(t)/2} x_i(0). \quad (43)$$

From Eqs. (41)–(43), and within the assumptions made above, it is straightforward to calculate the coarse grained expression for the first moments and the covariant matrix obtained using recursively the solution at each interval of time  $\tau$  between subsequent interruptions in the coupling constant. If  $m = l + 1$  is the number of interruptions and  $t = m\tau$ , we obtain

$$x_i(t) = e^{-m\Gamma(t)/2} x_i(0) \equiv e^{-b_\tau t/2} x_i(0), \quad (44)$$

$$\begin{aligned} \sigma_{22}(t) &= 2m \int_0^\tau dt' \Delta(t') + \sigma_{22}(0) e^{-m\Gamma(t)} \\ &= [\gamma_1(\tau) + \gamma_{-1}(\tau)]t + \sigma_{22}(0) e^{-b_\tau t}, \end{aligned} \quad (45)$$

where

$$b_\tau = \gamma_1(\tau) - \gamma_{-1}(\tau), \quad (46)$$

and  $\gamma_{\pm 1}(\tau)$  are given by Eq. (37). In terms of the Wigner function the solution has the same form as in Eqs. (20)–(21) and Eqs. (26)–(27), for  $r \ll 1$  and  $r \gg 1$ , respectively, with the substitutions  $N(t) \rightarrow \gamma_1(\tau)t$  and  $\Gamma(t) \rightarrow b_\tau t$ .

### 3.3. Comparison between the Shuttered Reservoir and the Nonselective Measurements Scenarios

It is straightforward to demonstrate that, in the shuttered reservoir scenario and for  $r \gg 1$ , the master equation whose solution we have presented above is the following

$$\begin{aligned} \frac{d\rho(t)}{dt} &= \gamma_1(\tau) \left[ a\rho(t)a^\dagger - \frac{1}{2}a^\dagger a\rho(t) - \frac{1}{2}\rho(t)a^\dagger a \right] \\ &+ \gamma_{-1}(\tau) \left[ a^\dagger \rho(t)a - \frac{1}{2}aa^\dagger \rho(t) - \frac{1}{2}\rho(t)aa^\dagger \right] \\ &+ \gamma_{-1}(\tau) \left[ a^\dagger \rho(t)a^\dagger - \frac{1}{2}a^{\dagger 2}\rho(t) - \frac{1}{2}\rho(t)a^{\dagger 2} \right] \\ &+ \gamma_{-1}(\tau) \left[ a\rho(t)a - \frac{1}{2}a^2\rho(t) - \frac{1}{2}\rho(t)a^2 \right]. \end{aligned} \quad (47)$$

In order to prove it one can, e.g., transform the master equation into a partial differential equation for the Wigner function (see, e.g., Appendix 12 of [34]), and then verify by direct substitution that the Wigner function solution satisfies the partial differential equation. Similarly one can see that, for  $r \ll 1$ , the master equation is given by the first two lines of Eq. (47).

Comparing Eq. (47), describing the dynamics in presence of an engineered shuttered reservoir, with Eq. (31), describing the dynamics in presence of nonselective energy measurements, one notices immediately that the difference between the two physical situations consists in the fact that while the nonselective measurements always set to zero the coherences, in the case of a shuttered reservoir the off diagonal elements of the density matrix do not vanish. The rate equations for the number probability distribution  $P_n(t)$  coincide in the off-resonant regime  $r \ll 1$  and are given in both cases by Eq. (34). In the resonant regime, on the contrary the contribution of the counter-rotating terms in the dynamics of  $P_n(t)$ , in the shuttered reservoir scenario, is non negligible. In this case, indeed the rate equation for  $P_n(t)$  contains the contribution of some off-diagonal elements of the density matrix too, these terms coming from the last two lines of Eq. (47).

This leads us to the following conclusions. In the off-resonant regime  $r \ll 1$ , whenever the initial state of the system is a Fock state, or any state which is diagonal in the Fock state basis, the system dynamics in presence of shuttered reservoirs coincides exactly with the dynamics in presence of nonselective energy measurements, since for this type of initial condition the density matrix, for the shuttered reservoir case, remains diagonal at all times  $t$ . Therefore, in this case, the shuttered reservoir mimics the dynamics in presence of nonselective energy measurements. This is interesting because it may be easier to realize experimentally a shuttered reservoir, instead of a sequence of nonselective energy measurements, by using reservoir engineering techniques as those used in the trapped ions context [1]. In [5, 9] we briefly discuss a possible implementation of the shuttered reservoir with trapped ions.

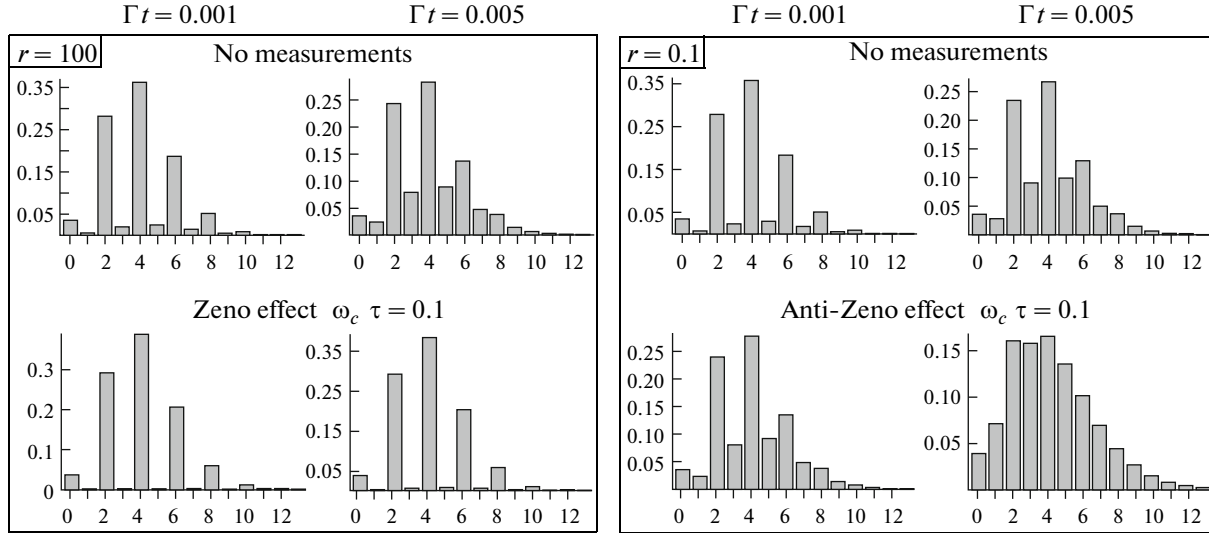


**Fig. 2.** Number probability distributions at different times  $t$  for the case of no measurements (upper row) and for the case of measurements with period  $\omega_c \tau = 0.1$  and  $r = 100$  (left) or  $r = 0.1$  (right), respectively.

Secondly, for a generic initial state, and for  $r \ll 1$  the time evolution of the number probability distribution, and therefore of all the observables which are diagonal in the Fock state basis, coincides for the two scenarios discussed in this paper. In Subsection 4.1 we will examine in detail the dynamics of the number probability distribution for the case of an initial Schrödinger cat state, and we will show that for certain values of the parameters one can manipulate the quantum-classical border prolonging or shortening the “life” of the cat.

Finally, in the resonant regime  $r \gg 1$ , a modulation of the system-reservoir interaction as, e.g., the one described in Eq. (39), modifies the decoherence of a Schrödinger cat state, as we will see in Subsection 4.2. However the modified dynamics differs from the one induced by a series of non-selective energy measurements because of the contribution of the counter-rotating terms present in the microscopic interaction Hamiltonian.

## 4. CONTROL OF THE QUANTUM-CLASSICAL BORDER

### 4.1. Evolution in Presence of Nonselective Energy Measurements

We begin considering the projective measurements scenario. We focus on the number probability distribution  $P_n$ . As noticed in Subsection 2.2, for an initial even coherent state of the form of Eq. (6), this quantity presents oscillations indicating the nonclassicality of the state (see Fig. 1). In presence of nonselective energy measurements  $P_n$  evolves according to Eq. (34) both in the resonant and in the off-resonant regime.

Following the lines of the Markovian derivation we solve directly Eq. (34) and obtain

$$P_n(t) = \frac{2\mathcal{N} e^{-\alpha^2}}{a_t + 1} \sum_{j=0}^n \frac{n!}{j![(n-j)!]^2} \left[ \frac{a_t}{a_t + 1} \right]^j \times \left[ \frac{\alpha^2 e^{-b_\tau t}}{(a_t + 1)^2} \right]^{n-j} \left\{ \exp \left[ \left( 1 - \frac{e^{-b_\tau t}}{a_t + 1} \right) \alpha^2 \right] + (-1)^{n-j} \exp \left[ - \left( 1 - \frac{e^{-b_\tau t}}{a_t + 1} \right) \alpha^2 \right] \right\}, \quad (48)$$

with  $b_\tau$  given by Eq. (46) and

$$a_t = \frac{\gamma_{-1}(\tau)}{b_\tau} [1 - e^{-b_\tau t}] \approx \gamma_{-1}(\tau)t. \quad (49)$$

The quantity  $a_t$  is the difference between the mean quantum number of the system oscillator at time  $t$ , whose dynamics is studied in [9], and the initial mean number of excitations.

In Fig. 2 we plot the behavior of the number probability distribution. These plots clearly show that the quantumness of the initial superposition, indicated by the absence of the odd number components, can be prolonged or shortened in time, by appropriate sequence of measurements. In more detail one can see that, in the resonant regime  $r \gg 1$ , i.e., when the frequency of the oscillator overlaps with the reservoir spectrum, measurements performed at times smaller than the reservoir correlation time  $\tau_R$  strongly inhibit the quantum to classical transition. On the contrary, in the off-resonant regime  $r \ll 1$  the anti-Zeno effect takes place and the decoherence of the Schrödinger

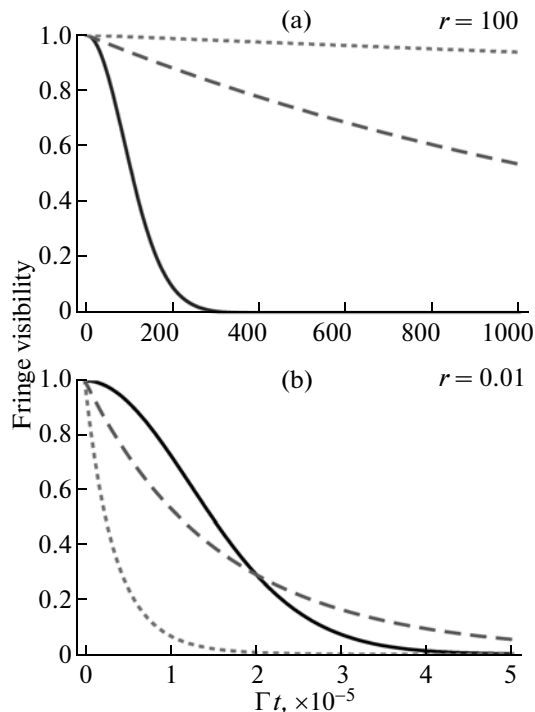


**Fig. 3.** Dynamics of the Wigner function peak for a high  $T$  Ohmic reservoir, and for an initial even coherent state with  $\alpha = 4$ , in correspondence of the parameters  $r = 100$  (a) and  $0.01$  (b). In both cases the solid line represents the Markovian dynamics in absence of shuttering. The dashed line corresponds to  $\omega_c\tau = 0.01$ , the dotted line corresponds to  $\omega_c\tau = 0.001$ .

cat state takes place at a much faster pace as a consequence of the energy measurements.

#### 4.2. Evolution in Presence of Shuttered Reservoir

We now focus on the shuttered reservoir scenario. Having in mind the Wigner function solution presented at the end of Subsection 3.2, we can calculate the fringe visibility function, defined by Eq. (24), when the system-reservoir coupling is modulated according to Eq. (39). The analytic expressions for  $F(\alpha, t)$  coincide with the ones given by Eqs. (25) and (28), for  $r \ll 1$  and  $r \gg 1$ , respectively, provided that the changes  $\Gamma(t) \rightarrow b_\tau t$  and  $N(t) \rightarrow \gamma_1(\tau)t$  are made.

For a high  $T$  reservoir, using Eqs. (12) and (38), we obtain the following analytic expression

$$\gamma_1(\tau) = \frac{\Gamma N(\omega_0)}{\tau \omega_c} \left\{ \omega_c \tau + \frac{1-r^2}{1+r^2} [1 - e^{-\omega_c \tau} \cos(\omega_0 \tau)] - \frac{2r}{1+r^2} e^{-\omega_c \tau} \sin(\omega_0 \tau) \right\}, \quad (50)$$

where  $\Gamma$  is given by Eq. (16).

When the shuttering period  $\tau$  is much longer than the reservoir correlation time, i.e.,  $\omega_c \tau \gg 1$ , one recovers the Markovian expression for the Wigner function peak dynamics in absence of shuttering. Stated another way, for  $\omega_c \tau \gg 1$  the shuttering does not affect the dynamics. On the other hand, for values of  $\tau$  such that  $\omega_c \tau \leq 1$ , one observes a change in the fringe visibility function depending on the behavior of the coefficient  $\gamma_1(\tau)$ , given by Eq. (50).

In Fig. 3 we compare the non-Markovian dynamics of the fringe visibility function, indicating the passage from a quantum superposition to a statistical mixture, in absence of shuttering and in presence of shuttering for,  $\omega_c \tau = 0.01$ , and  $\omega_c \tau = 0.001$ . For  $r = 100$  (Fig. 3a), i.e., in the resonant regime, the decay of  $F(\alpha, t)$  is inhibited by the shuttering events, and therefore the Schrödinger cat lives longer. This is a manifestation of the quantum Zeno effect. On the other hand, for  $r = 0.1$  (Fig. 3b), i.e., in the off-resonant regime, the fringe visibility function decays faster, indicating a rapid passage from a quantum superposition to a statistical mixture of the coherent states  $|\alpha\rangle$  and  $|\alpha\rangle$ . This is a manifestation of the anti-Zeno effect. In both cases, the shorter is  $\tau$ , the stronger is the inhibition or enhancement of the decay of  $F(\alpha, t)$  and therefore the most effective is the control of the quantum to classical transition. Summarizing, by manipulating the parameters of the engineered reservoir one can control the border between the quantum and the classical worlds.

## 5. SUMMARY AND CONCLUSIONS

In this paper we have investigated the non-Markovian short time dynamics of a quantum harmonic oscillator interacting with an engineered amplitude reservoir. We have derived a solution in terms of the Wigner function valid in two opposite physical regimes characterized by the parameters  $r \gg 1$  and  $r \ll 1$ . A comparison between the two solutions reveals that the counter-rotating terms present in the microscopic Hamiltonian model have a non-negligible effect in the resonant case. On the contrary, in the off-resonant case they can be neglected.

The availability of the simple analytic expressions describing short time dynamics of the system oscillator has allowed us to investigate the occurrence of the quantum Zeno and anti-Zeno effect. In particular we have focused on the dynamics of an initial Schrödinger cat state, i.e., a quantum superposition of two distinguishable coherent states. This state is strongly sensitive to decoherence induced by the external environment. The larger is the “separation” between the two components of the superposition, the faster is the decay into a statistical mixture of the two components.

Because of the fragility of such a state it is interesting to see whether it is possible to modify the decoherence induced by the environment by means of either nonselective measurements or modulation in the sys-

tem-reservoir coupling. Our results show that when the interval between the measurements (or the shuttering period)  $\tau$  is smaller than the reservoir correlation time  $\tau_R$ , then the passage from a quantum superposition to a classical statistical mixture may be controlled. In more detail one can inhibit or enhance the “life” of the Schrödinger cat, depending on some system/reservoir parameters. This result, which is based on the occurrence of the quantum Zeno or anti-Zeno effects, respectively, opens new possibility for protecting very fragile states like the Schrödinger cat states from the destructive effects of the external environment.

We have also proved that, in the off-resonant regime, one can mimic the effect of nonselective energy measurements by modulating the system-reservoir coupling constant. The second scenario might be easier to realize experimentally, and might therefore pave the way to experiments aimed at moving in a controlled way the quantum-classical border via the Zeno and anti-Zeno effect.

#### ACKNOWLEDGMENTS

The author acknowledges financial support from the Turku Collegium of Science and Medicine, Academy of Finland, the Emil Aaltonen Foundation, the Magnus Ehmrooth Foundation and the Väisälä Foundation. Stimulating discussions with Jyrki Piilo and Kalle-Antti Suominen are gratefully acknowledged.

#### REFERENCES

1. C. J. Myatt, B. E. King, Q. A. Turchette, C. A. Sackett, D. Kielpinski, W. M. Itano, C. Monroe, and D. J. Wineland, *Nature* **403**, 269 (2000).
2. Q.A. Turchette, C. J. Myatt, B. E. King, C. A. Sackett, D. Kielpinski, W. M. Itano, C. Monroe, and D. J. Wineland *Phys. Rev. A* **62**, 053507 (2000).
3. G. M. Palma, K.-A. Suominen, and A. K. Ekert, *Proc. R. Soc. London, Ser. A* **452**, 567 (1996); L. M. Duan and G. C. Guo, *Phys. Rev. Lett.* **79**, 1953 (1997); P. Zanardi and M. Rasetti, *Phys. Rev. Lett.* **79**, 3306 (1997); D. A. Lidar, I. L. Chuang, and K. B. Whaley, *Phys. Rev. Lett.* **81**, 2594 (1998); L. Viola and S. Lloyd, *Phys. Rev. A* **58**, 2733 (1988); D. Vitali and P. Tombesi, *Phys. Rev. A* **59**, 4178 (1999); L. Viola, E. Knill, and S. Lloyd, *Phys. Rev. Lett.* **85**, 3520 (2000); A. G. Kofman and G. Kurizki, *Phys. Rev. Lett.* **87**, 270405 (2001); M.S. Byrd and D. A. Lidar, *Phys. Rev. A* **67**, 012324 (2003).
4. P. Facchi, S. Tasaki, S. Pascazio, H. Nakazato, A. Tokuse, and D. A. Lidar *Phys. Rev. A* **71**, 022302 (2005).
5. S. Maniscalco, J. Piilo, and K.-A. Suominen, *Phys. Rev. Lett.* **97**, 130402 (2006).
6. B. Misra and E. C. G. Sudarshan, *J. Math. Phys.* **18**, 756 (1977).
7. A. M. Lane, *Phys. Lett. A* **99**, 359 (1983); W. C. Schieve, L. P. Horwitz, and J. Levitan, *Phys. Lett. A* **136**, 264 (1989); A. G. Kofman and G. Kurizki, *Nature (London)* **405**, 546 (2000); P. Facchi, H. Nakazato, and S. Pascazio, *Phys. Rev. Lett.* **86**, 2699 (2001); G. S. Agarwal, M. O. Scully, and H. Walther, *Phys. Rev. A* **63**, 044101 (2001).
8. P. Facchi and S. Pascazio, in *Progress in Optics*, Ed. by E. Wolf (Elsevier, Amsterdam, 2001), Vol. 42, Ch. 3, p. 147.
9. J. Piilo, S. Maniscalco, and K.-A. Suominen, *Phys. Rev. A* **75**, 032105 (2007).
10. M. C. Fischer, B. Gutierrez-Medina, and M. G. Raizen, *Phys. Rev. Lett.* **87**, 040402 (2001).
11. K. Koshino and A. Shimizu, *Phys. Rep.* **412**, 191 (2005).
12. U. Weiss, *Quantum Dissipative Systems* (World Sci., Singapore, 1999).
13. H.-P. Breuer and F. Petruccione, *The Theory of Open Quantum Systems* (Oxford Univ., Oxford, 2002).
14. R. P. Feynman and F. L. Vernon, *Ann. Phys. (N.Y.)* **24**, 118 (1963).
15. A. O. Caldeira and A. J. Leggett, *Physica A* **121**, 587 (1983).
16. F. Haake and R. Reibold, *Phys. Rev. A* **32**, 2462 (1985).
17. H. Grabert, P. Schramm, and G.-L. Ingold, *Phys. Rep.* **168**, 115 (1988).
18. B. L. Hu, J. P. Paz, and Y. Zhang, *Phys. Rev. D* **45**, 2843 (1992).
19. F. Intravaia, S. Maniscalco, and A. Messina, *Phys. Rev. A* **67**, 042108 (2003).
20. F. Intravaia, S. Maniscalco, and A. Messina, *Eur. Phys. J. B* **32**, 97 (2003).
21. S. Maniscalco, J. Piilo, F. Intravaia, F. Petruccione, and A. Messina, *Phys. Rev. A* **70**, 032113 (2004).
22. W. H. Zurek, *Rev. Mod. Phys.* **75**, 715 (2003).
23. J. P. Paz, S. Habib and W. H. Zurek, *Phys. Rev. D* **47**, 488 (1993).
24. S. Maniscalco, J. Piilo, F. Intravaia, F. Petruccione, and A. Messina, *Phys. Rev. A* **69**, 052101 (2004).
25. S. Maniscalco, F. Intravaia, J. Piilo, and A. Messina, *J. Opt. B: Quantum Semiclass. Opt.* **6**, S98 (2004).
26. M. S. Kim and V. Bužek, *Phys. Rev. A* **46**, 4239 (1992).
27. T. A. B. Kennedy and D. F. Walls, *Phys. Rev. A* **37**, 152 (1988).
28. M. S. Kim and V. Bužek, *Phys. Rev. A* **47**, 610 (1993).
29. A. Serafini, S. De Siena, F. Illuminati, and M. G. A. Paris, *J. Opt. B: Quantum Semiclass. Opt.* **6**, S591 (2004).
30. M. G. A. Paris, F. Illuminati, A. Serafini, and S. De Siena, *Phys. Rev. A* **68**, 012314 (2003).
31. G. Harel, A. G. Kofman, and A. Kurizki, *Opt. Express* **2**, 355 (1998).
32. G. S. Agarwal, *Phys. Rev. A* **61**, 013809 (1999).
33. J. Piilo and S. Maniscalco, *Phys. Rev. A* **74**, 032303 (2006).
34. S. M. Barnett and P. M. Radmore, *Methods in Theoretical Quantum Optics* (Oxford Univ., Oxford, 1997).